DOI: 10.1002/chem.200701976

Homo- and Heterodimetallic Geminal Dianions Derived from the Bis(phosphinimine) $\{Ph_2P(NSiMe_3)\}_2CH_2$ and the Alkali Metals Li, Na, and K

Katherine L. Hull,[a] Ian Carmichael,[b] Bruce C. Noll,[a] and Kenneth W. Henderson*[a]

Abstract: The geminal organodimetallic complexes $[(\{Ph_2P(NSiMe_3)\}_2C)_2M_4]$, where $M_4 = Na_4$, **3**; Li_2Na_2, **4**; $LiNa_3$, **5**; Li_2K_2, **6**; Na_2K_2, **7**, and Na_3K, **8**, have been prepared through a variety of methods including direct or sequential deprotonation of the neutral ligand with strong bases (*t*BuLi, *n*BuNa, $(Me_3Si)_2NNa$, $PhCH_2K$ or $(Me_3Si)_2NK$), transmetalation of the homometallic derivatives ($M_4 = Li_4$, **2** or Na_4, **3**) with *t*BuONa or *t*BuOK, and by cation exchange upon mixing the homometallic complexes in an arene solution. Complexes **3–8** have been characterized by single-crystal X-ray diffraction and are found to form a homologous series of dimeric structures in the solid-state, in accord with the previously reported structure of **2**. Each complex is composed of a plane of four metals, M_4, in which the ligands adopt capping positions to form distorted M_4C_2 octahedral cores. The metals in homometallic complexes **2** and **3** define an approximate square, whereas the heterometallic derivatives **4–8** have distinctly rhombic arrangements. The lighter metals in **4–8** interact strongly with the carbanions and the heavier metals are pushed towards the periphery of the structures. ^1H, ^{13}C, ^7Li, ^{31}P, and ^{29}Si multinuclear NMR spectroscopic studies, cryoscopic measurements, and electrospray ionization-mass spectroscopic studies are consistent with the dimers being retained in solution. Dynamic solution behavior was discovered for Li_2Na_2 complex **4**, in which all five possible tetrametallic derivatives Li_4, Li_3Na, Li_2Na_2, $LiNa_3$ and Na_4 coexist. Density functional theory (DFT) and natural bond order (NBO) calculations in association with natural population analyses (NPA) reveal significant differences in the electronic structures of the variously metalated dianions. The smaller cations are more effective in localizing the double negative charge on the carbanion (in the form of two lone pairs), leading to differences in the distribution of the electron density within the ligand backbones. In turn, a complex interplay of hyperconjugation, electrostatics and metal-ligand interactions is found to control the resulting electronic structures of the geminal organodimetallic complexes.

Keywords: alkali metals · carbanions · dianions · hyperconjugation · natural bond orbital analysis

Introduction

Research concerning geminal organodimetallic compounds (R_2CM_2) of the alkali metals can be traced back to the seminal synthesis of dilithiomethane by Ziegler in the mid 1950's.[1] The ensuing interest in this area was led primarily by West[2] and Lagow,[3] through investigations of polylithium organometallics prepared either by reaction of unsaturated organic compounds with alkyllithiums[4] or by metal-vapor synthesis.[5] In turn, this work laid the foundation for the multitude of synthetic uses of geminal organodimetallic complexes that are known today.[6,7]

Initial attempts to structurally characterize dilithiomethane were hampered by its instability, poor solubility, and high reactivity with air and moisture. However, Schleyer and Pople reported a theoretical analysis of dilithiomethane in 1976,[8] leading to a series of proposals predicting the possible oligomeric structures adopted by polylithium compounds.[9] Subsequent advances in synthetic methods[10,11] allowed the structural characterization of Li_2CD_2 by Stucky in 1990, using a combination of neutron and X-ray diffrac-

[a] K. L. Hull, Prof. B. C. Noll, Prof. K. W. Henderson
Department of Chemistry and Biochemistry
University of Notre Dame, Notre Dame, IN 46556-5670 (USA)
Fax: (+1) 574-631-6652
E-mail: khenders@nd.edu

[b] Prof. I. Carmichael
Department of Chemistry and Biochemistry
and the Radiation Laboratory
University of Notre Dame, Notre Dame, IN 46556-5670 (USA)

Supporting information for this article is available on the WWW under http://www.chemeurj.org/ or from the author.

tion data of powder samples.[12] These studies showed that Li_2CD_2 forms the antifluorite structure known for Li_2O[13] and Be_2C.[14]

The problematic issues surrounding the structural characterization of dilithiomethane have proven to be representative of this class of compounds in general. As a result, very few geminal organodimetallics have been crystallographically characterized in the solid state. Prior to our recent communication,[15] there were only three structurally characterized, homoleptic, geminal organodimetallic compounds containing alkali metals in the literature: the bis(phosphineimine) $[(\{Ph_2P(NSiMe_3)\}_2CLi_2)_2]$,[16,17] the nitrile $[\{Me_3Si(NC)CLi_2\}_{12}\cdot 6\,Et_2O]$,[18] and the polymer 9,9-dilithiofluorene $[C_{13}H_8Li_2\cdot THF]_\infty$.[19] This group of complexes was recently added to by the report of the bis(thiophosphinoyls) $[(\{Ph_2P(S)\}_2CLi_2\cdot Et_2O)_2]$ and $[(\{Ph_2P(S)\}_2CLi_2)_2\cdot 3\,Et_2O]$.[20] In addition, there are a handful of mixed-anion complexes that contain geminal dianionic ligands. To date, these compounds include the sulfone $[\{PhSO_2(Me_3Si)CLi_2\}_6\cdot Li_2O\cdot 10\,THF]$,[21] the sulfoximine $[\{Ph(MeN)SO(Ph)CLi_2\}_4\cdot Li_2O\cdot 6\,THF]$,[22] the phosphonate $[(\{(MeO)_2PO(Me_3Si)CLi_2\}_3\cdot Me_2N)_2\cdot(Li\cdot 2\,TMEDA)_2]$,[23] the phosphiminine $[\{Me_2P(NSiMe_3)CH\}_6\cdot\{Me_2(Bu)SiO\}_2\cdot Li_{14}]$,[24] and the mixed-metal complex $[\{(Me_3SiCH_2)_3Al\}_2\cdot(H_2CLi_2)]$.[25]

All of these crystallographically characterized complexes contain dilithiated carbanions, and we have been interested for some time in preparing geminal organodimetallic derivatives of the heavier alkali metals.[26] Such complexes are interesting on several fronts. First, given the lack of direct data available on their characterization it is reasonable to question if it is even possible to form geminal organodimetallics of the heavier metals. Indeed, their synthesis may be inhibited by either steric or electronic effects. In this regard, it is worth noting that caution should be applied when assuming the formation of geminal dianions simply based on the analysis of quenched products, owing to the possible participation of quasi-dianion complexes.[27,28] Another appealing feature of studying the heavier alkali metal derivatives is that most of the theoretical studies to date have focused upon dilithiated complexes. Hence, little is known regarding the effects of the countercation (gegenion) on the electronic structure of the dianions.[29] Finally, from a synthetic utility perspective, changing the alkali metal cation is very likely to have significant consequences on the reactivity and selectivity of these reagents, and this type of metal tuning has not yet been exploited.[6,30]

Our previous attempts at preparing single crystals of sodium and potassium geminal organodimetallic complexes by using a variety of heteroatom-substituted methylene ligands have proven to be problematic.[26] In particular, the issue of poor solubility that is well-known for many dilithiated complexes, is commonly exacerbated for the heavier alkali metal derivatives. We decided to revisit the use of the bis(phosphinimine) ligand bis-*N*-diphenyl-trimethylsilylphosphiniminomethane, **1**,[31] which was successfully applied to the synthesis of $[(\{Ph_2P(NSiMe_3)\}_2CLi_2)_2]$, **2**, by Cavell and Stephan.[16,17] This ligand was attractive for our purposes, as it is known to form geminal dimetallic complexes of not only Li_2, but also of Al_2,[32] Pb_2,[33] Sn_2,[33] Cr_2,[34] Zn_2,[35] and Li/Rh.[36] In addition, this ligand has been shown to form stable "C=M" carbenes supported by single metal centers such as Pt,[37] Ti,[38] Zr,[21,39] Sm,[40] Hf,[41] Mo,[42] Ge,[43,44] Ca,[45] and Ba.[46]

We recently reported in a preliminary communication the syntheses of $[(\{Ph_2P(NSiMe_3)\}_2CNa_2)_2]$, **3**, and $[(\{Ph_2P(NSiMe_3)\}_2CLiNa)_2]$, **4**, the first examples of geminal organodimetallic compounds containing a heavy alkali metal to be structurally characterized.[15] In this paper, we outline a comprehensive study of these complexes and extend this series through the synthesis of the unsymmetrical Na_3Li complex $[(\{Ph_2P(NSiMe_3)\}_2C)_2LiNa_3]$, **5**. We also outline the synthesis and characterization of the first authenticated potassium-containing geminal organodimetallic complexes, $[(\{Ph_2P(NSiMe_3)\}_2CLiK)_2]$, **6**, $[(\{Ph_2P(NSiMe_3)\}_2CNaK)_2]$, **7**, and $[(\{Ph_2P(NSiMe_3)\}_2C)_2Na_3K]$, **8**. We present detailed solid-state structural comparisons and solution analyses of this set of compounds. The unexpected synthesis and structural characterization of the mixed-metal, mixed-anion complex $[(\{Ph_2P(NSiMe_3)\}_2CH)\{(Me_3Si)_2N\}NaK\cdot tol]$, **9**, is also described. Finally, a density functional theory (DFT) computational study, including natural bond orbital (NBO) analysis, was completed to provide insights into the energetics and electronic structures of the homo- and heterodimetallic compounds.

Results and Discussion

Synthesis: The original syntheses of dilithio complex **2** required either extended reaction times (three days using PhLi)[16] or application of excess base (15 equivalents and 12 h using MeLi).[17] We found that **2** can be conveniently prepared in essentially quantitative yield by reaction of two molar equivalents of *t*BuLi with the parent ligand **1** in arene solution at ambient temperature within 1.5 h. The formation of **2** under these conditions was confirmed by in situ ^1H NMR monitoring of a reaction conducted in $[D_6]$benzene and comparing the spectrum produced with an authentic sample of crystalline **2**. Initial attempts to prepare the disodio analogue **3** using either NaH or NaHMDS failed, giving solely the monosodiated product.[47] Replacement of these reagents with the very strong base *n*BuNa proved successful.[48] ^1H NMR monitoring of the reaction of two molar equivalents of *n*BuNa with **1** in $[D_6]$benzene at ambient temperature showed complete conversion to the dianion within a few minutes (as determined by disappearance of the methylene/methine triplet).

An alternative strategy to prepare the disodio complex by transmetalation of **2** with excess *t*BuONa resulted in the unexpected preparation of the mixed-metal Li_2Na_2 complex **4**. Subsequent structural and computational studies of this system give some insight into the stabilization of **4** towards further metal exchange (see later). In turn, **4** was also prepared by sequential metalation of the parent ligand **1** by

using sodium hexamethyldisilazide (NaHMDS) followed by *t*BuLi. However, reversing the order of addition of the bases yielded the monolithiated product. Presumably this is a consequence of the lower basicity of the sodium amide compared with the alkyllithium reagent. Complex **4** can also be prepared by mixing the homometallic dianions **2** and **3** in arene solution.

Finally, the Na_3Li complex **5** was prepared from the reaction of **1** with *n*BuNa and *t*BuLi in a 2:3:1 molar ratio in toluene solution. This unsymmetrical complex is the major component of the crystalline material produced, but is co-crystallized along with both the Na_4 complex **3** and Li_2Na_2 complex **4**. A summary of the successful strategies to prepare the sodium-containing complexes is outlined in Scheme 1.

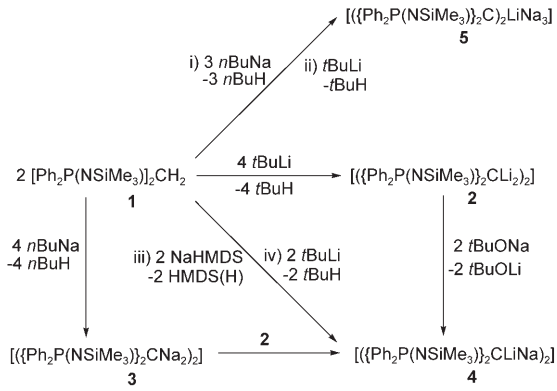

Scheme 1. Synthetic routes to the sodium-containing geminal dimetallics.

With this synthetic information in hand we moved on to attempt the preparation of the potassium derivatives. The synthesis of the mixed-metal complexes was achieved, although some differences were noted compared with the Li/Na systems. Similarities include, the preparation of the Li_2K_2 complex **6** both by transmetalation of **2** with *t*BuOK, as well as by sequential metalation of **1** with KHMDS followed by *t*BuLi (reversing the order again results in monolithiation). Also, the Na_2K_2 complex **7** was prepared from the reaction of the Na_4 complex **3** with *t*BuOK. However, efforts to synthesize **7** by sequential metalation proved more complex than those for **4**. Reaction of ligand **1** with NaHMDS followed by benzylpotassium (BnK) produced the unexpected mixed-metal, mixed-anion species [({Ph_2P-$(NSiMe_3)$}$_2$CH){$(Me_3Si)_2N$}NaK·Tol], **9**, which contains both monometalated bis(phosphinimine) and hexamethyldisilazide. In contrast, reaction of **1** with KHMDS followed by *n*BuNa produced the monopotassiated species.[39b] Clearly, these efforts to doubly deprotonate **1** are hampered by the presence of HMDS(H) during the reaction, that is, the second equivalent of metal base is preferentially reacting with the free amine instead of the monometalated ligand. To avoid this issue the monopotassiated complex was prepared by the equimolar reaction of **1** and either K metal, KHMDS, BnK, or *n*BuK, followed by crystallization and isolation as the pure solid. This complex was then re-dissolved in fresh toluene and reacted with one molar equivalent of *n*BuNa to successfully yield the Na_2K_2 complex **7**.

Increasing the molar ratio of *n*BuNa present in this reaction resulted in the precipitation of the Na_3K complex **8**. Hence, partial transmetalation takes place with expulsion of the more electropositive metal from the dianionic ligand. Attempts to isolate the dipotassiated complex were hampered by its high reactivity. In situ ^{1}H NMR monitoring of the reactions of ligand **1** with excess BnK in [D_8]thf, [D_6]benzene, and [D_8]toluene indicated only monometalation of the ligand. Replacement of BnK with the stronger base *n*BuK showed complete disappearance of the methylene triplet in [D_6]benzene, suggesting that the ligand had been doubly deprotonated. However, an identical reaction run in protio-benzene was monitored using no-D NMR, and showed an identical set of resonances, but with the inclusion of a triplet at $\approx$1.8 ppm.[49] Therefore, it is likely that the dipotassiated complex is indeed formed as a transient species, which quickly deprotonates the solvent (benzene) to form the monopotassiated complex. A summary of the successful strategies to prepare the potassium-containing complexes is outlined in Scheme 2.

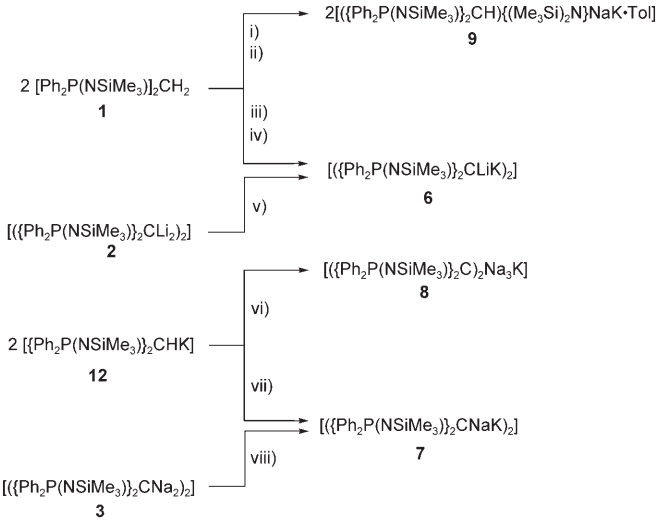

Scheme 2. Synthetic routes to the potassium-containing complexes. i) 2 NaHMDS; ii) 2 BnK, −Tol; iii) 2 KHMDS, −2 HMDS(H); iv) 2 *t*BuLi, −2 *t*BuH; v) 2 *t*BuOK, −2 *t*BuOLi; vi) 3 *n*BuNa, −2 *n*BuH, −*n*BuK; vii) 2 *n*BuNa, −2 *n*BuH; v) 2 *t*BuOK, −2 *t*BuONa.

Solid-state structural studies: Single-crystal X-ray analyses were successfully completed on compounds **3**–**9**. Data for compound **9** is located in the Supporting Information for brevity. Although crystallography established that the $LiNa_3$ complex **5** was present, it co-crystallized in almost equimolar quantities with the Li_2Na_2 complex **4** and further minor contamination with Na_4 complex **3**. The Na_3K complex **8** was also found to contain a minor component ($\approx$7%) of the Na_2K_2 complex **7**. The whole-molecule disorder in these

cases manifests itself most notably as partial-site disorder of the metal positions. Therefore, discussion of the metrical parameters involving **5** and **8** should be regarded with due caution. Nevertheless, the gross structures of all seven geminal dimetallic compounds **2**–**8** are not in doubt, and are displayed in Figure 1. Table 1, Table 2 and Table 3 summarize a series of key bond length and angle data for the complexes.

All form "dimers" (with respect to the ligands) in which the two W-shaped, NPCPN, bis(phosphinimine) ligands lie in a staggered conformation relative to one another. The four metals of each complex form a plane within the core of the structures. This is in contrast with the majority of tetrametallic alkali metal complexes, in which the metals normally adopt a tetrahedral relationship to one another within cubane frameworks.[50] Looking in more detail at the gross structures it becomes apparent that there are significant differences present as a result of changing the countercations. Four values are useful in analyzing the distortions within the complexes: i) the improper N-P-P-N torsion angle can be used as a guide to the linearity of the backbones, ii) the angle made between the two P–C–P planes of the separate ligands indicates their twist from perpendicularity, iii) the internal M–M–M ring angles show the distortion from square arrangements, and iv) the N–P–C(*ipso*) angles give an indication of the tilting of the phenyl rings (Table 3).

The homometallic complexes **2** and **3** are clearly the most symmetrical structures, and possess approximately octahedral M_4C_2 cores (Figure 2). They have nearly linear ligand backbones, which are also almost perfectly perpendicular to one another. This results in a square arrangement for the

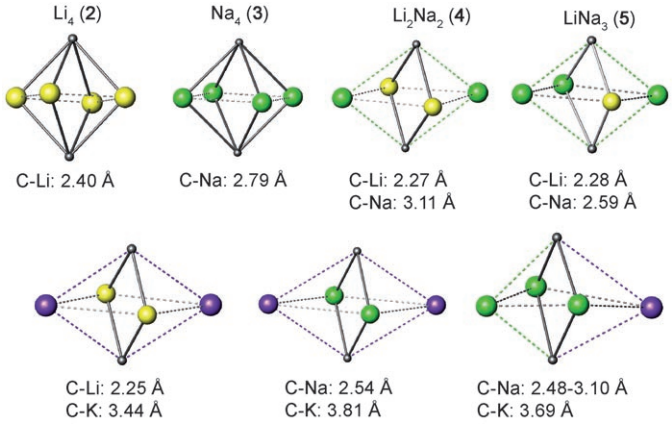

Figure 2. Central dianionic carbon-metal octahedral core for each of the structurally characterized geminal organodimetallic compounds (**2**–**8**). Mean carbon-metal bond lengths are given for the M_4 and $M^1{}_2M^2{}_2$ complexes, and ranges are given for the $M^1{}_3M^2$ complexes as these distances vary more widely.

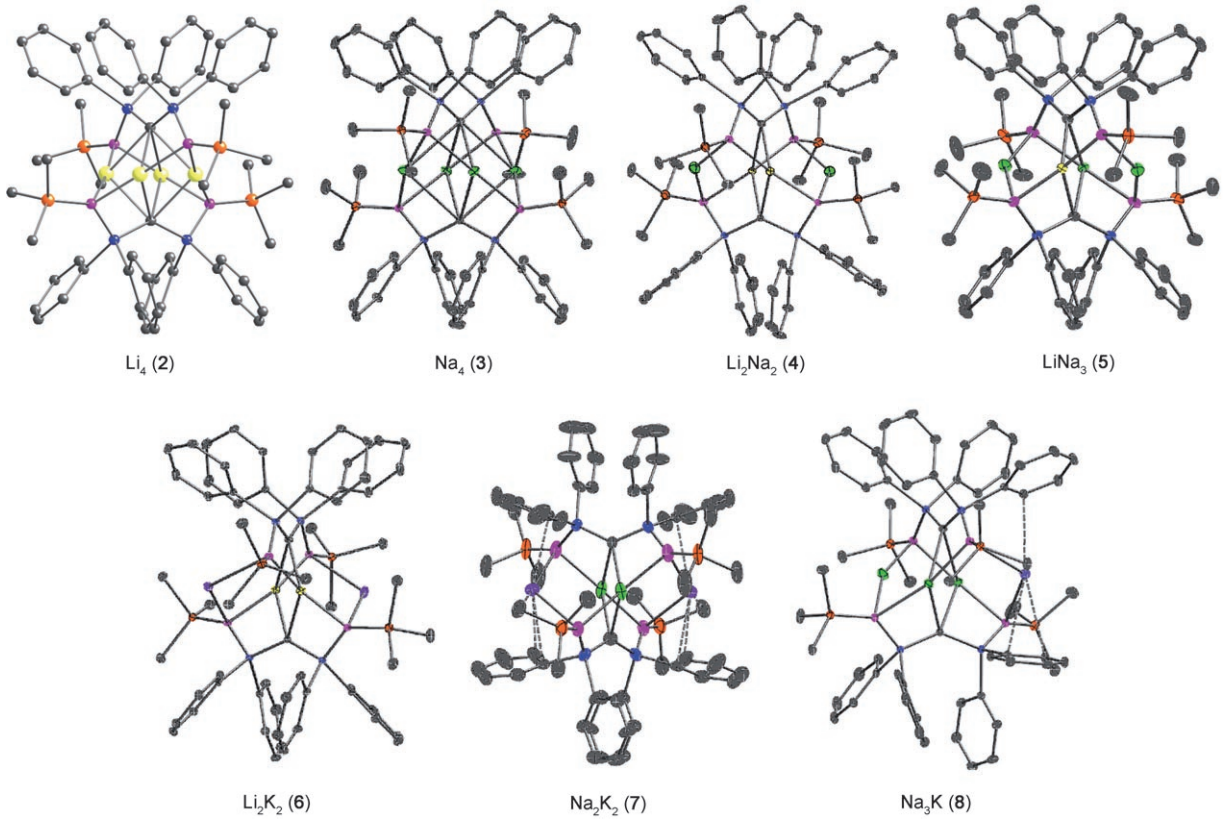

Figure 1. Crystal structures for the geminal organodimetallic compounds **2**–**8** (the structure of **2** is reproduced from the data collected in ref. [16]). Thermal ellipsoids are drawn at 50% probabilities. Solvents of crystallization and hydrogen atoms have been removed for clarity. Cation-π interactions are shown as dotted lines in **7** and **8**. Only the major component of the structures of **5** and **8** are shown. Li: Yellow, Na: green, K: purple, C: black, P: blue, N: pink, Si: orange.

Table 1. Selected bond lengths [Å] for **2**–**8**.

	C–P	P–N	N–Si	C–Li	C–Na	C–K	N–Li	N–Na	N–K
Li_4 (**2**)[a]	1.687(3)	1.621(3)	1.715(3)	2.348(7)	–	–	2.068(7)	–	–
	1.694(3)	1.628(3)	1.719(3)	2.348(7)			2.073(7)		
	1.696(3)	1.629(3)	1.724(3)	2.356(6)			2.086(6)		
	1.700(3)	1.632(2)	1.726(3)	2.357(6)			2.100(6)		
				2.417(7)			2.132(6)		
				2.438(7)			2.143(6)		
				2.441(7)			2.143(6)		
				2.451(7)			2.145(6)		
Na_4 (**3**)	1.6881(9)	1.6100(8)	1.6923(8)	–	2.7420(10)	–	–	2.3234(9)	–
	1.6891(9)	1.6137(8)	1.6981(8)		2.7559(10)			2.3255(10)	
	1.6901(9)	1.6167(8)	1.6960(8)		2.8503(11)			2.3849(9)	
	1.6937(9)	1.6177(8)	1.7043(8)		2.8578(10)			2.3941(9)	
					2.7230(10)				
					2.7346(10)				
					2.8210(10)				
					2.8422(11)				
Li_2Na_2 (**4**)	1.6752(10)	1.6109(9)	1.6965(10)	2.229(2)	3.0214(11)	–	2.116(2)	2.3925(12)	–
	1.6772(10)	1.6127(9)	1.6960(9)	2.259(2)	3.1152(12)		2.123(2)	2.4078(11)	
	1.6773(11)	1.6159(10)	1.6997(9)	2.278(2)	3.1530(11)		2.134(2)	2.4207(10)	
	1.6778(12)	1.6168(9)	1.7084(10)	2.295(2)	3.1575(12)		2.135(2)	2.4403(10)	
$LiNa_3$ (**5**)	1.6793(19)	1.6098(16)	1.6968(17)	2.245(6)	2.594(3)	–	2.102(6)	2.042(16)	–
	1.6828(19)	1.6144(16)	1.6984(16)	2.269(6)	2.595(3)		2.117(6)	2.054(16)	
	1.6833(19)	1.6147(16)	1.6985(17)	2.287(14)	2.689(18)		2.289(15)	2.280(3)	
	1.6839(19)	1.6187(16)	1.7018(16)	2.312(14)	2.691(16)		2.382(15)	2.302(3)	
					2.870(2)			2.3782(17)	
					2.926(2)			2.3873(18)	
					3.1656(21)			2.3892(18)	
					3.2022(21)			2.4034(17)	
Li_2K_2 (**6**)	1.6795(15)	1.6051(13)	1.6937(13)	2.221(3)	–	3.3557(15)	2.093(3)	–	2.7816(13)
	1.6828(15)	1.6067(13)	1.6967(12)	2.240(3)		3.4234(15)	2.095(3)		2.8154(13)
	1.6834(15)	1.6140(12)	1.6979(13)	2.254(3)		3.4382(15)	2.105(3)		2.8680(12)
	1.6856(14)	1.6137(13)	1.7025(13)	2.277(3)		3.5494(15)	2.123(3)		2.9013(13)
Na_2K_2 (**7**)	1.664(2)	1.604(4)	1.685(3)	–	2.532(4)	3.8071(30)	–	2.420(3)	2.851(3)
	1.667(2)	1.608(3)	1.689(3)		2.543(5)	3.8101(26)		2.445(3)	2.868(3)
Na_3K (**8**)	1.6729(15)	1.6055(13)	1.6839(13)	–	2.5015(16)	3.6000(15)	–	2.3333(14)	2.8338(14)
	1.6834(15)	1.6112(13)	1.6863(13)		2.5549(16)	3.9406(16)		2.3731(15)	2.8683(13)
	1.6851(15)	1.6129(13)	1.6972(13)		2.6365(16)			2.3750(15)	
	1.6856(15)	1.6231(13)	1.6983(13)		2.6945(16)			2.4708(14)	
					2.890(2)				
					3.1192(21)				

[a] ref. [17]

metals, with no significant tilting of the phenyl groups. The heterodimetallic complexes show varying degrees of distortion, owing to the distinct positions adopted by the two pairs of cations. As seen in Figure 2, the metals within complexes **4**–**8** adopt planar rhombic arrangements, with the more acute angles associated with the heavier metals.

The lighter metals form relatively close contacts with the carbons, whereas the more electropositive metals are pushed towards the exterior of the structures. Moreover, the M–C distances in the homo- and heterometallic complexes vary considerably. Mixing the metals results in the M–C distances shortening significantly for the lighter metal and lengthening for the heavier metal. To illustrate, the mean M–C distances in the homometallic Li_4 and Na_4 complexes **2** and **3** are 2.394(7) and 2.791(1) Å. In comparison, the average Li–C and Na–C distances in the Li_2Na_2 complex **4** are 2.265(2) and 3.112(1) Å. These deviations from the homometallic complexes are partly a consequence of electrostatic repulsions of the four metals within the M_4 planes. Specifically, movement of the heavier, softer metals away from the carbanion allows the smaller, harder metals to move closer to the negatively charged centers. In addition, the carbanions in the symmetrical heterometallic structures **3**, **6** and **7** can be considered as only four coordinate (two C–P contacts and two C–M contacts), as the larger metals are now pushed away from the core of the complexes. This reduction in coordination number also allows closer interactions with the remaining two metal centers. The two inner

Table 2. Selected bond angles [°] for **2**–**8**.

	P–C–P	C–P–N	C–P–C(ipso)	N–P–C(ipso)	P–N–Si
Li_4 (**2**)[a]	132.3(2)	104.14(14)	112.98(15)	109.78(14)	131.0(2)
	132.7(2)	104.17(13)	113.1(2)	110.24(14)	131.9(2)
		104.55(13)	113.27(15)	110.31(2)	132.0(2)
		104.69(14)	113.9(2)	110.34(14)	132.2(2)
			114.36(14)	110.62(10)	
			114.0(2)	110.89(14)	
			114.7(2)	110.94(14)	
			114.9(2)	111.04(14)	
Na_4 (**3**)	128.36(5)	108.10(4)	112.22(4)	106.93(4)	131.77(5)
	129.76(6)	108.39(4)	112.75(5)	108.14(5)	134.58(5)
		108.42(4)	112.86(4)	108.24(4)	134.84(5)
		108.69(4)	112.94(5)	108.45(4)	139.89(6)
			114.18(5)	108.83(4)	
			114.41(5)	108.85(4)	
			114.52(4)	108.93(4)	
			114.66(5)	109.10(5)	
Li_2Na_2 (**4**)	134.33(6)	106.45(5)	112.65(5)	108.71(5)	133.79(6)
	134.79(6)	106.54(5)	112.85(5)	108.92(5)	133.40(6)
		106.95(5)	113.03(5)	109.13(5)	137.99(6)
		107.25(5)	113.65(6)	109.48(5)	139.05(6)
			114.91(5)	109.76(5)	
			115.26(5)	110.11(5)	
			115.79(5)	110.27(5)	
			115.91(5)	110.30(5)	
$LiNa_3$ (**5**)	131.27(11)	106.57(9)	113.08(9)	108.43(9)	131.19(11)
	131.91(12)	107.06(9)	113.35(9)	108.79(8)	135.17(11)
		107.09(9)	113.41(9)	108.99(8)	136.19(11)
		107.11(9)	113.75(9)	109.45(8)	136.86(11)
			113.86(9)	109.53(9)	
			113.99(9)	109.80(8)	
				110.23(9)	
				110.53(9)	
Li_2K_2 (**6**)	132.21(9)	107.44(7)	112.46(7)	108.49(7)	132.66(8)
	133.18(9)	107.48(7)	113.57(7)	108.83(7)	133.43(8)
		107.57(7)	113.61(7)	109.42(7)	137.30(8)
		107.81(7)	114.43(7)	109.89(7)	139.56(8)
			114.82(7)	110.07(7)	
			113.90(7)	110.11(7)	
			114.57(7)	110.90(7)	
			116.14(7)	110.77(7)	
Na_2K_2 (**7**)	133.1(3)	110.5(2)	111.83(9)	104.71(19)	139.9(2)
	134.0(4)	111.20(19)	112.95(11)	105.12(15)	140.5(2)
			113.7(3)	105.82(14)	
			117.6(2)	116.9(3)	
Na_3K (**8**)	131.08(9)	108.39(7)	113.18(7)	104.45(7)	133.68(8)
	134.75(9)	109.17(7)	113.19(7)	105.86(7)	137.34(8)
		110.31(7)	113.58(7)	107.17(7)	139.79(9)
		111.71(7)	113.60(7)	108.52(7)	141.28(8)
			113.97(7)	108.93(7)	
			114.03(7)	109.08(7)	
			114.18(7)	109.56(7)	
			114.26(7)	112.43(7)	

[a] ref. [17]

metals are tetracoordinate, binding to two carbanions and to a nitrogen on each ligand, whereas the outer metals are only two coordinate, through contacts to a nitrogen on each ligand. The strong interactions between the inner two metals and the carbanions are likely the reason for the transmetalation reactions ceasing at the heterometallic constitutions despite the addition of excess *t*BuONa or *t*BuOK.

The adjustment of the heterometallic complexes from square to rhombic arrangements of the metals also affects the relative positions adopted by the two bis(phosphinimine) backbones. In particular, the deviation of the metal plane from square leads to narrowing of the angle made between the P–C–P planes of the two ligands. This is most clearly observed in complexes **6** and **7**, which have the P–C–P planes intersecting at angles of 74.86(9) and 66.91(6)° respectively. This pivoting of the ligands is required to retain strong M–N interactions with the larger pair of metals that are situated further away from the carbanions. Indeed, only relatively small variations of <0.12 Å are found for the individual mean M–N distances between the homo- and heterometallic complexes. The introduction of two different metals also leads to twisting of the ligand backbones. As seen from Table 3, the N-P-P-N dihedral angles are $<5°$ for the homometallic complexes **2** and **3**, but reach up to 61.17(34)° for the Na_2K_2 complex **7**. These twists are again a consequence of maintaining close M–N interactions between the nitrogen centers of the ligand and the smaller, more Lewis acidic, metal cations.

Another clear difference between the complexes is the orientation of the phenyl rings (Figure 1). In particular, the phenyl rings in the potassium-containing complexes **7** and **8** are folded towards the heavier, two-coordinate, metals on the periphery of the structures to accommodate cation-π interactions.[51] This is seen in the

Table 3. Descriptive metrical parameters [°] within **2**–**8**.

		N–P–P–N	P–C–P planes intersect	M–M–M	N–P–C(ipso) range
Li_4	(**2**)[a]	2.42/2.88	89.51	86.0(3), 86.0(3) 93.8(3), 94.3(2)	109.78(14) –111.04(14)
Na_4	(**3**)	3.24(6)/4.47(7)	89.01(6)	85.91(2), 86.35(2), 86.94(3), 93.51(2)	106.93(4)–109.10(5)
Li_2Na_2	(**4**)	14.13(7)/23.02(7)	87.69(4)	57.62(6), 59.07(6) 121.37(7), 121.85(9)	108.71(5)–110.30(5)
$LiNa_3$	(**5**)	4.47(12)/7.27(12)	88.50(13)	65.92(13), 66.90(13), 103.10(5), 124.07(21)	108.43(9)–110.53(9)
Li_2K_2	(**6**)	3.90(9)/10.05(9)	74.86(9)	48.73(6), 50.90(7), 129.71(8), 130.63(8)	108.49(7)–110.77(7)
Na_2K_2	(**7**)	56.64(34)/61.17(34)	66.91(6)	52.95(4), 127.05(4)	104.71(19)–116.9(3)
Na_3K	(**8**)	9.43(10)/48.11(10)	77.86(8)	57.24(2), 71.84(4), 112.03(3), 116.17(3)	104.45(7)–112.43(7)

[a] ref. [17]

N–P–C(ipso) angles, which vary over a wide range for the heterometallic complexes **7** and **8**, and also from the relatively close potassium-phenyl ring contacts (e.g. $K–C_{ipso}$ 3.072(3) and 3.071(3) Å in **7**). The unsymmetrical Na_3K complex **8** is interesting as two distinct ligand types are incorporated within a single aggregate. One of the ligands has an approximately planar backbone, whereas the other is significantly twisted, with N-P-P-N torsion angles of 9.43(10) and 48.11(10)°, respectively.

The twisting of the ligand backbones does not significantly affect the C–P, P–N, or N–Si bond lengths. Indeed, the individual mean bond lengths within the ligands of **2**–**8** vary by $\leq$0.04 Å. This is a key finding when considering the electronic structure of the anionic ligands. Also, although only small differences are found between the bond lengths of the ligands, it is notable that the Li_4 complex **2** and the Na_2K_2 complex **7** are on each end of the ranges (lightest and heaviest set of metal complexes). In particular, the mean C–P, P–N, and N–Si bond lengths are longer in **2** (1.694(3), 1.628(3), and 1.721(3) Å) and shorter in **7** (1.666(2), 1.606(4), 1.687(3) Å). The structural differences again suggest small, but discernible effects on the bonding depending upon the type of alkali metal present. This gegenion effect will be dealt with in more detail in the theoretical section.[52]

Finally, the previous crystallographic characterizations of the neutral ligand $\{Ph_2P(NSiMe_3)\}_2CH_2$[31] **1**, and the monometalated complexes $[\{Ph_2P(NSiMe_3)\}_2CHLi]$,[47a] **10**, $[\{Ph_2P(NSiMe_3)\}_2CHNa]$,[47a] **11** and $[\{Ph_2P(NSiMe_3)\}_2CHK]$,[39] **12** allow structural comparisons to be made. The main features of relevance with respect to the bonding within the ligand backbones are the mean C–P and P–N bond lengths. The neutral ligand has the longest C–P and the shortest P–N bond lengths (1.825(1) and 1.536(2) Å), the monometalated ligands are intermediate (mean 1.727(4) and 1.586(3) Å), and the dimetalated are the shortest of the set (mean 1.683(2) and 1.615(2) Å). Therefore, the increase in charge on the ligand has significant structural consequences beyond the local bonding environment of the carbanion.

Solution studies: ^1H, ^{13}C, ^7Li, ^{29}Si, and ^{31}P NMR spectroscopic data for the dimetalated compounds **2, 3**, **4**, **6**, and **7** as solutions in $[D_8]$toluene are provided in Table 4. With the exception of Li_2Na_2 complex **4** (see later), all of the spectra display a single set of signals at ambient temperature. The Na_4 complex **3** was chosen as a representative sample and subjected to a ^1H NMR spectroscopic variable-temperature study between 25 and −80 °C. A single set of signals were present at all temperatures within this range, with the chemical shift positions varying by $<$0.1 ppm (Figure S2 in the Supporting Information). In combination, these data are consistent with a single solution species being present. This analysis is further supported by cryoscopic measurements of **3** in benzene. Molecular weights of 1269(±16) and 1348(±13) g mol^{-1} were determined in 0.0525 and 0.0993 M solutions. These values correspond very well with dimeric aggregation (theoretical 1205 g mol^{-1}), as found in the solid state. Examining the chemical shift values in Table 4 in detail, it can be seen that only relatively small changes are observed between the complexes. One point of particular interest is the location of the ^{13}C signal for the carbanion centers in **3**, **6**, and **7**. This signal could not be located in the previously characterized Li_4 complex **2**. This is a common occurrence for geminal dianions, and was rationalized as a consequence of signal broadening associated with attachment to lithium centers.[16,17] We were similarly unable to locate this signal for **2** or for Li_2Na_2 complex **4**, despite the use of extended acquisition times and running samples at varying field strengths. However, this signal could be located for complexes **3**, **6**, and **7**. The chemical-shift positions for these three signals are similar to the value of δ = 37.84 ppm found for the neutral ligand **1**, and are shifted downfield compared with the monometalated complexes **10**–**12** (δ = 22.9 ppm,

Table 4. Multinuclear NMR data [ppm] for the dimetalated compounds.

		^1H			^{13}C		^7Li	^{29}Si	^{31}P
		o-Ph	*m*-, *p*-Ph	$SiMe_3$	C-anion	$SiMe_3$			
Li_4	(**2**)	7.48	6.96	0.00	not obs.	4.39	–	–	14.43
Na_4	(**3**)	7.44	6.90	−0.04	40.99	4.32	–	–15.35	7.56
Li_2Na_2	(**4**)	7.51	6.96	0.09	not obs.	–	0.58	−12.86	14.60
Li_2K_2	(**6**)	7.73–7.62	7.10–6.88	0.23	33.50	5.57	0.22	−16.44	6.71
Na_2K_2	(**7**)	7.81–7.27	6.96	0.12	38.04	5.50	–	−19.94	3.95

[D_6]benzene; 27.5 ppm, [D_6]benzene; 22.1 ppm, [D_8]thf) respectively).[39a,47b]

The Li_2Na_2 complex **4** is observed to have more complex solution behavior than the other dianions. The trimethylsilyl region of the ^{1}H NMR spectrum of **4** in [D_8]toluene clearly indicated the presence of five distinct signals at $\delta = 0.09$, 0.05, 0.03, 0.00, and -0.04 ppm. The two signals at $\delta = 0.00$ and -0.04 ppm are readily assigned as the previously characterized Li_4 and Na_4 complexes **2** and **3**, respectively. It was presumed that the remaining three signals result from the Li_2Na_2, Li_3Na, and $LiNa_3$ mixed-metal complexes. In an effort to confirm this assignment a series of spiking experiments were undertaken. Specifically, 1:1, 3:1, and 1:3 mixtures of **2** and **3** were dissolved in [D_8]toluene and their ^{1}H NMR spectra recorded. Figure 3 shows each of these

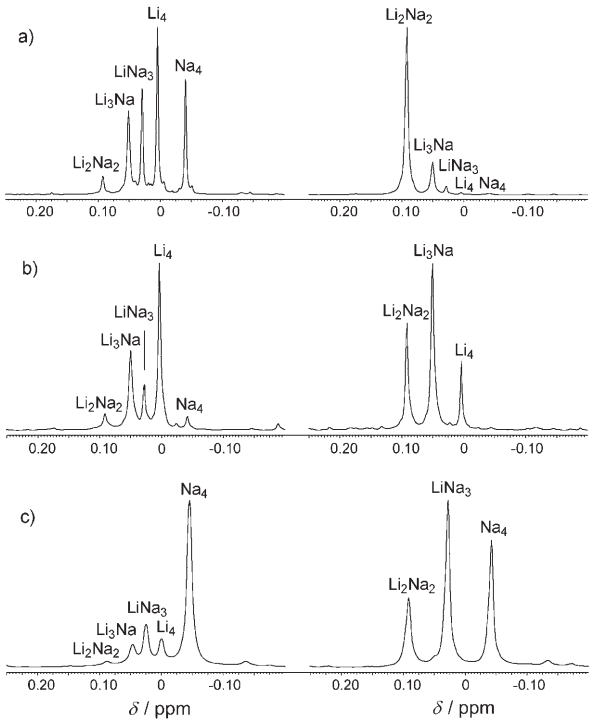

Figure 3. In situ ^{1}H NMR spectra of the trimethylsilyl resonances on mixing: a) 1:1, b) 3:1, and c) 1:3 equivalents of **2** and **3** in [D_8]toluene. The spectra on the left are taken within 15 minutes of mixing, and the spectra on the right are at equilibrium.

spectra after a few minutes and then again at equilibrium. Analysis of these spectra clearly establishes the identities of the Li_2Na_2, Li_3Na, and $LiNa_3$ mixed-metal complexes in solution at $\delta = 0.09$, 0.05, and 0.03 ppm respectively.

It is evident from the coexistence of all five solution species that there is relatively little energetic difference between them. A further point of note arising from this study is that the heterometallic complexes may be prepared by mixing the homometallic precursors. This indicates that a dynamic exchange of the metals is occurring between the complexes. Indeed, the spectra were observed to take several hours or even days to reach an eventual equilibrium distribution of the complexes, indicating relatively slow exchange of the metals.

Electrospray ionization-mass spectrometry (ESI-MS) of selected dimetalated compounds in THF further support the formation of dimeric aggregates. All negative-ion mode spectra of the dimetalated compounds showed the presence of a mass envelope corresponding to $[L_2M_3]^-$ ($L = \{Ph_2P(NSiMe_3)\}_2C^{2-}$) dimers with one metal removed. A typical spectrum is shown in Figure 4 for the Na_4 complex **3**. Larger

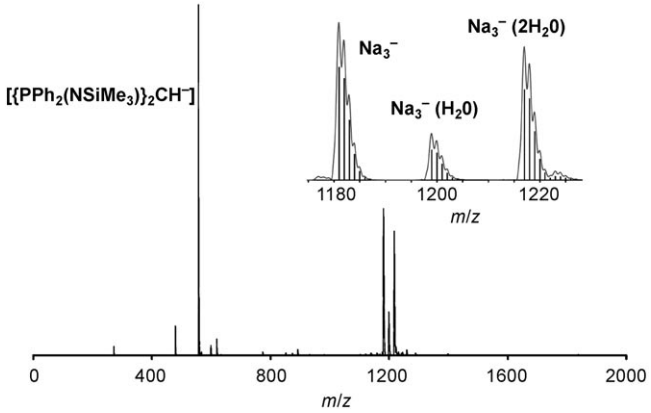

Figure 4. ESI-MS of Na_4 complex **3** in THF (negative-ion mode). The individual solid lines represent the calculated isotopic distributions.

m/*z* signals are also observed, owing to the stoichiometric reactions of the complexes with water, which presumably occur inside the electrospray chamber. For **3**, signals corresponding to the reaction with one and two water molecules are observed. These species are most likely a result of the partial hydrolysis products $[\{L\}\cdot\{LH\}\cdot NaOH\cdot Na_2]^-$ and $[\{LH\}_2\cdot\{NaOH\}_2\cdot Na]^-$. The most abundant signal in most spectra is the singly-protonated ligand $[LH]^-$ at *m*/*z* 557. This again is likely a product of partial hydrolysis of the highly reactive anions.

It is interesting that a small signal at *m*/*z* 579 is found in the spectrum of **3**, which corresponds with the monomer $[\{Ph_2P(NSiMe_3)\}_2CNa]^-$. This indicates that, although the major species present is the dimer, in accord with the NMR and cryoscopic studies, the monomer is present in small amounts in the mass spectrometer.

As expected, the mixed-metal complexes **4**, **6**, and **7** display more complex spectra. A section of a typical spectrum of Li_2Na_2 complex **4** is shown in Figure 5. Signals corresponding to Li_3^- and Li_2Na^- are present, in addition to the partial hydrolysis products. Again, the major species present appear to be dimeric. An interesting feature in the spectra of the mixed-metal complexes is that the highest m/z signals contain a pair of lighter metals and a single heavier metal, that is, Li_2Na^- in **4**. This suggests that the heavier metal ions are more readily removed from the complexes to produce the ions in the mass spectrometer. The removal of the heavier ion of the pair is consistent with the solid-state studies, in

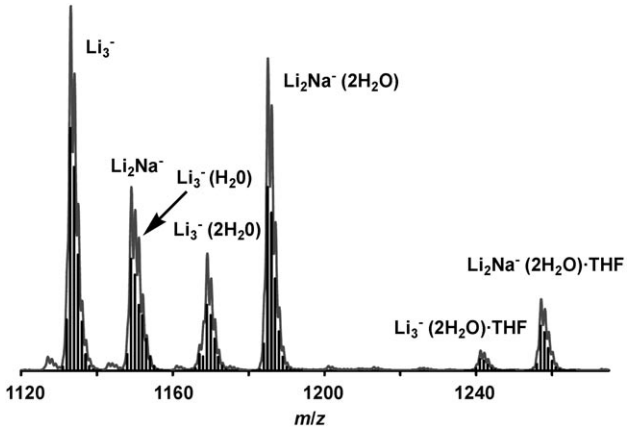

Figure 5. Section of the ESI-MS of Li_2Na_2 complex **4** in THF (negative-ion mode). The individual solid lines represent the calculated isotopic distributions.

which these cations are located on the periphery of the molecules. Also, the more ionic metals would be expected to interact more weakly with the dianions and be more easily removed.

Theoretical studies: A computational investigation was undertaken with three main aims: i) to determine the relative energies of the homo- and heterometallic complexes, ii) to assign the electronic structure of the dianions, and iii) to discern any effects of altering the metal ions present.

Geometry optimizations were carried out at the B3LYP/6-31G* level of theory on the full molecules $[(\{Ph_2P(NSiMe_3)\}_2C)_2M_4]$ ($M_4 = Li_4$, **I**; Na_4, **II**; K_4, **III**; Li_2Na_2, **IV**; Li_2K_2, **V**; Na_2K_2, **VI**; Li_3Na, **VII**, and $LiNa_3$, **VIII**). The crystallographic coordinates of the relevant complexes were used as starting positions. The dipotassio calculation **III** was started by using the coordinates of the disodio structure after replacing the metals. The full molecules were used in these instances to mimic the experimental structures as completely as possible. In turn, these calculations should provide reasonable estimations of the relative energies between the complexes. The smaller model complexes $[(\{H_2P(NSiH_3)\}_2C)_2M_4]$ ($M_4 = Li_4$, **IX**; Na_4, **X**; K_4, **XI**; Li_2Na_2, **XII**; Li_2K_2, **XIII**, and Na_2K_2, **XIV**) were then geometry optimized at the B3LYP/6-311G** level of theory, and used for the natural population analyses (NPA) and natural bond order (NBO) analyses.

First, the optimized geometries of the full molecules **I**–**VI** correspond well with the appropriate crystal structures (Tables S1 and S2 in the Supporting Information). The mean C–M and N–M bond lengths vary by <0.11 Å between theory and experiment. Similarly, the mean C–P, P–N, and N–Si bond lengths are very well reproduced, varying by <0.04 Å compared to the crystal structures. The mean bond angles within the ligand backbones generally vary by $<3°$ between theory and experiment. The exception is the Na_4 complex **II**, in which two of the metals extend out from the center of the core to form a more rhombic metal plane, similar to the mixed-metal aggregates. Moreover, this distortion is relatively minor, with the largest difference being an increase in the mean N–P–C(ipso) angle by 6.2°. Overall, the geometries of the calculated structures compare very well with the experimental data.

Scheme 3 details the theoretical reaction thermicities on forming the heterometallic complexes from the homometallic precursors. In all cases the reactions are predicted to be

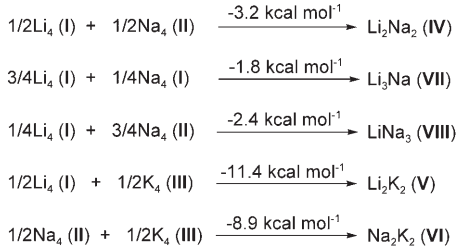

Scheme 3. Calculated thermicities of mixed-metal product formation.

energetically favorable, in line with the experimental results from the transmetalation reactions. The reactions involving the mixed Li and Na complexes are close to being thermoneutral, with the largest energy is -3.2 kcal mol^{-1} for the conversion of the homometallic complexes **I** and **II** to Li_2Na_2 complex **IV**. This is in accord with the NMR investigations, which show the coexistence of all five possible Li/Na dimeric combinations. In comparison, the formation of Li_2K_2 and Na_2K_2 (**V** and **VI**) from the homometallic complexes is predicted to be substantially more exothermic (-8.9 and -11.4 kcal mol^{-1}). Again, this is reflected in their NMR data, which indicate the presence of only single heterometallic solution species.

Recent independent theoretical investigations by Klobukowski,[53] Mézailles[20] and Harder[45] have addressed the electronic structure of bis(phosphinimine)-stabilized geminal dianions (or the closely related bis(thiophosphinoyl) species).[54] Findings of importance are: i) the -2 charge remains largely localized at the central carbanion in the form of two lone pairs, ii) the individual atomic centers are highly charged in the form $Si^{\delta+}$-$N^{\delta-}$-$P^{\delta+}$-$C^{\delta-}$-$M^{\delta+}$, iii) single $P-C_{(anion)}$ and P–N bonds are present, and iv) the $P-C_{(anion)}$ distances decrease and the remaining bond lengths at phosphorous increase upon deprotonation of the ligand. The change in the bond lengths upon deprotonation have been rationalized as a consequence of either substantial negative hyperconjugative contributions between the two lone pairs of the carbanion and the adjacent stabilizing groups, or alternatively through the formation of strong electrostatic interactions on the ligand backbone.[20,45,53,55] Studies thus far have solely focused on dilithiated complexes. Our variously metalated systems provide the opportunity to examine the bonding situation from a unique perspective. The electronic structures of the model complexes **IX**–**XIV** were therefore geometry optimized (Table 5 and Table 6) and studied using NPA and NBO analyses (Table 7).

Table 5. Mean bond lengths [Å] for model complexes **IX–XIV**.

		C–Li	C–Na	C–K	C–P	P–N	N–Si	P–H	Si–H	N–Li	N–Na	N–K
ligand		–	–	–	1.835	1.539	1.697	1.422	1.491	–	–	–
Li_4	(**IX**)	2.385	–	–	1.690	1.644	1.728	1.432	1.492	2.079	–	–
Na_4	(**X**)	–	2.764	–	1.693	1.642	1.721	1.436	1.495	–	2.406	–
K_4	(**XI**)	–	–	3.198	1.695	1.635	1.709	1.442	1.499	–	–	2.766
Li_2Na_2	(**XII**)	2.305	2.847	–	1.689	1.641	1.724	1.434	1.493	2.107	2.406	–
Li_2K_2	(**XIII**)	2.280	–	3.271	1.688	1.634	1.716	1.437	1.495	2.102	–	2.794
Na_2K_2	(**XIV**)	–	2.591	3.458	1.689	1.635	1.711	1.439	1.497	–	2.436	2.759

Table 6. Mean bond angles [°] for model complexes **IX–XIV**.

		P–C–P	C–P–H	C–P–N	P–N–Si	N–P–H
ligand		112.36	101.61	112.81	151.76	118.67
Li_4	(**IX**)	132.96	117.28	103.45	127.77	110.55
Na_4	(**X**)	125.76	116.11	108.33	126.42	109.22
K_4	(**XI**)	118.89	115.09	111.87	126.93	108.64
Li_2Na_2	(**XII**)	130.71	116.68	105.65	127.33	110.11
Li_2K_2	(**XIII**)	129.66	116.27	106.83	128.11	110.16
Na_2K_2	(**XIV**)	125.30	115.57	109.66	128.51	109.28

All of the calculations show a consistent pattern with respect to the location of two inequivalent lone pairs at the carbanion; one sp^2 hybridized orbital directed towards the M_4 plane and one pure p orbital perpendicular to the ligand plane (Figure 6 and Table S3 in the Supporting Information). Each nitrogen carries two lone pairs, and the Wiberg bond indices show single C–P and P–N bonds (Table S4 in the Supporting Information). This analysis is also consistent with the general pattern of the natural charges within the molecules (Table 7, Table S5 and Table S6 in the Supporting Information). Taking the Na_4 calculation **X** as an example, the carbanions and nitrogen centers carry high negative charges of −1.731 and −1.652, whereas the phosphorous and silicon centers carry positive charges of 1.348 and 1.065 respectively. Overall, this leads to the Lewis structure shown in Figure 7.

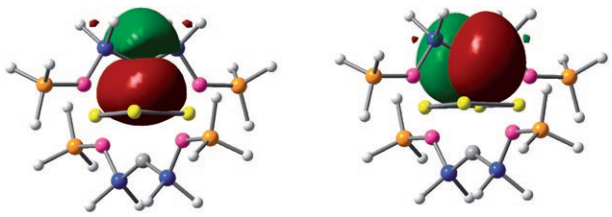

Figure 6. View of the sp^2 and p lone pairs on one carbanion of Li_4 complex **IX** generated from the NBO analysis.

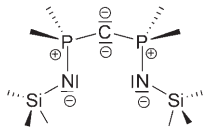

Figure 7. Localized Lewis structure of the dianionic ligand.

The main finding is that varying the metal counter cation has remarkably little effect on the metrical parameters of the ligands in **IX–XIV** (Table 5 and Table 6). This is exemplified by the small difference in bond lengths across the series of ligands, being $\leq$0.021 Å. Nevertheless, small but discernible trends are seen between the metalated complexes. Overall, the bond lengths from Li_4 complex **IX** to K_4 complex **XI** show shortening of the P–N and N–Si bonds by 0.009 and 0.019 and Å, and lengthening of the C–P, P–H and Si–H bonds by 0.005, 0.010, and 0.007 Å. In all cases, Na_4 complex **X** has intermediate values, and generally intermediate values are also found for the mixed-metal complexes **XII–XIV**. These patterns cannot be explained solely by either a hyperconjugative or an electrostatic bonding model. Increased hyperconjugative interactions of the carbanion lone pairs would be expected to decrease the C–P bonds, with concomitant lengthening of the P–N and P–H bonds. Also, the varying differentials in adjacent atomic charges found from the NPA analyses would be predicted to result in lengthening of the C–P and P–N bonds, and shortening of the P–H and Si–H bonds, on moving from **IX–XI**. Clearly, neither isolated bonding model neatly fits the available data. Another factor to be incorporated when comparing these very small changes in bond lengths is the polarizing effect of the metals. The smaller, more Lewis acidic the metal ion is, the stronger it will interact with surrounding electron density. In turn, this leads to a relative lengthening of the bonds for the ligands involving the lighter metals. Overall, the observed changes in bond lengths between the various metalated complexes **IX–XIV** appear to be a conse-

Table 7. Mean natural charges on each atom in model complexes **IX–XIV**.

		C	P	H_P	N	Si	H_{Si}	Li	Na	K
ligand		−1.033	1.407	−0.068	−1.518	1.109	−0.199	–	–	–
Li_4	(**IX**)	−1.804	1.360	−0.082	−1.665	1.072	−0.192	0.875	–	–
Na_4	(**X**)	−1.731	1.348	−0.095	−1.652	1.065	−0.198	–	0.890	–
K_4	(**XI**)	−1.688	1.350	−0.113	−1.646	1.065	−0.207	–	–	0.923
Li_2Na_2	(**XII**)	−1.776	1.361	−0.091	−1.654	1.071	−0.196	0.842	0.920	–
Li_2K_2	(**XIII**)	−1.765	1.368	−0.101	−1.647	1.073	−0.201	0.827	–	0.960
Na_2K_2	(**XIV**)	−1.713	1.365	−0.107	−1.660	1.079	−0.206	–	0.862	0.950

quence of multiple, competing, and sometimes counteracting effects.[55]

Analysis of the NPA charges within **IX–XIV** does show substantial movement of the electron density depending upon the metal present. Taking the Li_4, Na_4, and K_4 models **IX–XI** as a series, all of the metals have positive charges near unity, which increase slightly with size (0.875, 0.890, 0.923 in **IX**, **X**, and **XI** respectively). In contrast, the negative charge on the carbanions decreases as the metals become larger (−1.804, −1.731, −1.688 in **IX**, **X**, and **XI**, respectively). The alkali metals are well known to localize charge in monoanions through electrostatic stabilization.[52] The smaller, more highly polarizing ions are more efficient at this localization of charge. This additional electron density for the heavier metal complexes flows mainly to the four P–H bonds of the ligands (charges on H_P are −0.082, −0.095, and −0.113 in **IX**, **X**, and **XI**).

The trends in the variation in bond lengths observed in the model complexes are generally reproduced in the calculations of the full molecules (Table S1 in the Supporting Information). The Li_4 and K_4 complexes **I** and **III** have distances on each end of the bond length ranges, with Na_4 complex **II** and the mixed-metal derivatives having intermediate distances. One notable difference between the model complexes and the calculations of the full molecules is that the mean C-P distance decreases from 1.713 to 1.686 Å in **I** and **III** (compared with a moderate increase of 0.005 Å from **IX** to **XI**). However, the pattern of decreasing C–P and P–N bond lengths in association with incorporation of the heavier metals is consistent with the experimental data, in which Li_4 and Na_2K_2 complexes **2** and **7** represent the two limiting cases (Table 1). It is likely that the significant changes in both the sterics and the electronics in the full molecules are sufficient to reverse some of the trends found for the metrical parameters of the model complexes. In particular, delocalization of the charge into the aromatic rings is likely to have a substantial effect.

Conclusion

The synthesis and characterization of complexes **3–8** significantly expands the class of homo- and heterodimetallic geminal dianion complexes incorporating the alkali metals. The synthesis of mixed-metal Li/Na, Li/K and Na/K complexes by using the bis(phosphinimine) ligand demonstrates its flexibility and general utility for the preparation of novel types of complexes. This ligand combines two properties that have emerged to be important for the successful synthesis and stabilization of geminal dianions: adequate residual acidity of the monometalated complex, and sufficient steric protection of the resulting metal complex. However, attempts to prepare and isolate the dipotassiated derivative led to reaction of the presumed intermediate with the solvent media. This suggests that a limitation in stability, likely arising from the destabilization of the structure, has been reached for the dianion of this system.

Varying the metal or combination of metals within the complexes is seen to have subtle consequences on the gross structures adopted. In particular, although all of the complexes are composed of two W-shaped N-P-C-P-N bis(phosphiminine) ligands capping a plane of four metals, the structures differ in the arrangement of the metals and the relative positions adopted by the ligands. The mixed-metal complexes are less symmetrical, with a rhombic rather than a square arrangement of the metals, and with the ligands skewed rather than perpendicular to each other. Furthermore, the backbones of the ligands in the heterodimetallic complexes indicate that they may distort from planarity without undue effects on the local bonding. Therefore, all of the bonds in the ligand are essentially single bonds, as a resonance delocalized structure would require planarity within the backbone.

The solution NMR, cryoscopic, ESI-MS, and computational studies all support the retention of dimeric aggregation, as found in the solid state. The mixed Na/Li complexes undergo dynamic exchange in solution, where an equilibrium mixture containing all five possibilities of metal combinations within dimers is observed, that is, Li_4, Na_4, Li_2Na_2, Li_3Na, and $LiNa_3$. Computational studies suggest that there is little energetic difference between these complexes, allowing all five to co-exist, with the Li_2Na_2 complex dominating. No such equilibria are apparent in solutions that contain the Li_2K_2 and Na_2K_2 derivatives, and the computational studies point to a strong enthalpic preference for the 2:2 mixed-metal combinations.

Finally, an analysis of the various metalated complexes, both by experiment and theory, indicates that the electronic structures of the ligands are only slightly affected by the type of alkali metal present. This is not to be confused with the importance of having a metal present. The cations localize the −2 charge on the carbanion (in the form of two lone pairs), and they are very likely critical in the stabilization of the dianion. Indeed, this view is supported by our inability to isolate the dipotassiated complex. In addition, analysis of this set of complexes has allowed unique insights into the nature of the bonding present in the dianionic ligand backbones. Changing the countercation results in substantial variations in the electron density distributions within the ligands in which the lighter metals more effectively localize the charge at the carbanion. The effects on the remainder of the ligand may be explained by a subtle interplay of hyperconjugative interactions, electrostatics, and the influence of metal polarization. It also appears that the organic substituents attached to the backbone of the ligand play an important role in the fine tuning of the final electronic structure of the dianions. Present work is directed towards the characterization of charge-separated geminal dianion intermediates as a means to gain further understanding of the bonding within these unusual molecules.

Experimental Section

General Procedures: All operations were carried out by using Schlenk techniques or inside an argon-filled glove box.[56] All glassware was flame-dried under vacuum before use. *t*BuLi (1.7 M) was purchased from Aldrich and stored at 4 °C. Benzylpotassium and *n*BuNa were synthesized according to literature procedures.[48] *t*BuONa (Lancaster, 97 %), *t*BuOK (Fluka, 97 %), NaHMDS (Acros, 97 %), and KHMDS (Aldrich, 95 %) were purchased and used as received. Toluene and hexane were dried by passage through copper-based catalyst and molecular-sieve columns (Innovative Technology). Anhydrous benzene (Alfa Aesar, 99.8 %) was purchased and stored over 4 Å molecular sieves. Deuterated solvents were purchased from Cambridge Isotope Laboratories, and were dried by storage over 4 Å molecular sieves. The ^{1}H, ^{7}Li, ^{13}C, ^{29}Si, and ^{31}P NMR spectra were recorded on Varian-300/500 or Bruker Avance-800 spectrometers at 25 °C. The ^{1}H and ^{13}C NMR spectra were referenced internally to the residual signals of the deuterated solvents. The ^{7}Li, ^{29}Si, and ^{31}P spectra were referenced to external samples of 1 M LiCl in D_2O, 1 M TMS in [D_8]toluene, and 1 M H_3PO_4 in D_2O set at 0 ppm. IR spectra were recorded by means of a Nicolet Avatar 360 FTIR spectrophotometer through KBr plates as Nujol mulls. Melting points were recorded by means of a Meltemp apparatus. Elemental analyses were performed by Midwest Microlab, LLD, but proved problematic owing to the high air- and moisture-sensitivity of the samples and also as a consequence of the partial removal of solvents of crystallization upon isolation. Mass spectra were recorded on a Micromass Quatro triple LC quadrupole mass spectrometer.

X-ray Crystallography: Single crystals were examined under Infineum V8512 oil. The datum crystal was affixed to either a thin glass fiber atop a tapered copper mounting pin or Mitegen mounting loop and transferred to the 100 K nitrogen stream of a Bruker APEX II diffractometer equipped with an Oxford Cryosystems 700 series low-temperature apparatus. Cell parameters were determined using reflections harvested from three sets of 12×0.5° ω scans. The orientation matrix derived from this was transferred to COSMO[57] to determine the optimum data collection strategy requiring a minimum of 4-fold redundancy. Cell parameters were refined by using reflections harvested from the data collection with $I>10\sigma(I)$. All data were corrected for Lorentz and polarization effects, and runs were scaled by using SADABS.[58] Table 8 lists the key crystallographic parameters for **3**–**9**.The structures were solved from partial datasets by using the Autostructure option in APEX 2.[57] This option employs an iterative application of the direct methods, Patterson synthesis, and dual-space routines of SHELXTL[59] followed by several iterative cycles of least squares refinement. Hydrogen thermal parameters were set to 1.2× the equivalent isotropic U of the parent atom, 1.5× for methyl hydrogens. Final refinement was performed against all data harvested from data collection. Details on individual refinements, including descriptions of disorder, can be found in the cif files CCDC (**4**), 670729 (**5**) 670726 (**6**) 670728 (**7**) 670727 (**8**) and 670730 (**9**). These data can be obtained free of charge from The Cambridge Crystallographic Data Centre via www.ccdc.cam.ac.uk/data_request/cif.

Computational details: The Gaussian 03 series of programs was used for the calculations.[60] Geometry optimizations of the full molecules **I–XIV** were performed by using density functional theory with the B3LYP functional[61] and the standard polarized split-valence, 6-31G*, basis set.[62] No symmetry constraints were imposed and the molecules were allowed to freely optimize by using related crystal structure data as starting geometries. The geometries of the model complexes **IX–XIV** were geometry optimized with a more flexible basis set[63] at the B3LYP/6-311G** level of theory,[62] and used for the natural bond order (NBO)[64] and natural population analyses (NPA).[65] These geometries were verified as true minima by using frequency analyses.

[({$Ph_2P(NSiMe_3)$}$_2CNa_2$)$_2$], 3: The phosphinimine (0.559 g, 1.0 mmol) was placed inside a nitrogen-filled Schlenk tube and dissolved on the addition of 10 mL of dry benzene. The solid base *n*BuNa (0.168 g, 2.10 mmol) was

Table 8. Selected crystal data for **3**–**9**.

	3	**4**	**5**	**6**	**7**	**8**	**9**
formula	$C_{74}H_{88}N_4Na_4P_4Si_4$	$C_{74}H_{88}Li_2N_4Na_2P_4Si_4$	$C_{74}H_{88}Li_{1.36}N_4Na_{2.64}P_4Si_4$	$C_{74}H_{88}K_2Li_2N_4P_4Si_4$	$C_{31}H_{39}KN_2NaP_2Si_2$	$C_{76}H_{92}K_{1.07}N_4Na_{2.93}P_4Si_4$	$C_{44}H_{65}KN_3NaP_2Si_4$
F_w	1361.68	1329.58	1339.86	1361.8	619.85	1406.97	872.38
T [K]	100(2)	100(2)	100(2)	100(2)	100 (2)	100(2)	123(2)
crystal system	triclinic	triclinic	triclinic	triclinic	monoclinic	triclinic	triclinic
space group	$P\bar{1}$	$P\bar{1}$	$P\bar{1}$	$P\bar{1}$	$C2/c$	$P\bar{1}$	$P\bar{1}$
a [Å]	12.3275(2)	14.5700(6)	12.0869(5)	10.9579(6)	14.2301(6)	11.9692(4)	11.0168(9)
b [Å]	17.0832(3)	14.5952(6)	17.0782(6)	13.3605(7)	26.6172(11)	13.8278(4)	11.7602(10)
c [Å]	19.6578(4)	18.6933(8)	19.6111(7)	25.2938(14)	19.2254(8)	25.4664(8)	22.3520(18)
α [°]	101.4513(10)	91.530(3)	99.917(2)	92.877(3)	90	78.8325(18)	103.276(5)
β [°]	103.1949(10)	105.048(2)	103.382(2)	97.879(3)	94.873(2)	78.8605(17)	90.130(4)
γ [°]	103.7451(10)	104.295(2)	103.497(2)	90.874(3)	90	71.1639(18)	117.058(5)
V [Å^3]	3772.64(12)	3702.4(3)	3718.4(2)	3662.6(3)	7255.6(5)	3874.7(2)	2490.9(4)
Z	2	2	2	2	4	2	2
ρ [Mg m^{-3}]	1.199	1.193	1.197	1.235	1.205	1.206	1.163
μ ($Mo_{K\alpha}$) [mm^{-1}]	0.229	0.222	0.224	0.326	0.338	0.276	0.308
crystal size [mm^{-1}]	0.25 ×0.25 ×0.15	0.29 ×0.28 ×0.22	0.49 ×0.31 ×0.20	0.27 ×0.08 ×0.08	0.35 ×0.26 ×0.16	0.32 ×0.10 ×0.10	0.43 ×0.41 ×0.25
T_{max}/T_{min}	0.97/0.94	0.95/0.94	0.96/0.90	0.97/0.92	0.91/0.95	0.97/0.98	0.88/0.34
θ range [°]	1.10–31.50	1.13–0.94	1.110–24.96	0.81–28.39	1.53–25.62	1.57–28.56	0.94–26.35
refln. coll.	241 599	300 720	65 640	90 391	47 237	103 530	25 514
ind. refln.	24 877	38 148	12 944	18 333	6695	19 258	14 843
R(nt)	0.0343	0.0512	0.0266	0.0434	0.0328	0.0372	0.0591
obs. refln. [$I>2\sigma(I)$]	21 266	24 855	10 930	14 788	5061	15 339	12 610
GOF on F^2	1.04	1.057	1.081	1.011	1.021	1.037	1.497
R_1,wR_2 [$I>2\sigma(I)$]	0.0324, 0.0848	0.0404, 0.0929	0.0355, 0.0891	0.0356, 0.0820	0.0568, 0.1455	0.0382, 0.0888	0.0673, 0.1767
R_1, wR_2 (all data)	0.0408, 0.0921	0.0878, 0.1195	0.0463, 0.1010	0.0501, 0.0892	0.0858, 0.1827	0.0549, 0.0966	0.0863, 0.1988
largest peak/hole [e Å^{-3}]	0.566/−0.394	0.863/−0.592	0.738/−0.437	0.468/−0.305	1.057/−1.184	0.787/−0.702	0.680/−0.589

added slowly to the solution through a solids addition tube at ambient temperature. The mixture was stirred for 30 min until complete dissolution occurred. The volume of the solution was reduced in vacuo until precipitation ensued. The mixture was then heated to afford a clear yellow solution. Cooling to ambient temperature resulted in the formation of yellow crystals (isolated yield: 0.414 g, 69%). The resulting compound was highly air-sensitive and required manipulation inside an argon-filled glove box. The crystals decomposed without melting above 200°C. The complex crystallizes with two benzene molecules per dimer, as determined by X-ray crystallography. These molecules are partially removed on evacuation. ^{1}H NMR (500 MHz, [D$_8$]toluene, 25°C): δ=7.44 (m, 16H; *o*-H), 6.90 (m, 24H; *m*-, *p*-H), −0.04 ppm (s, 36H; CH_3Si); ^{13}C{^{1}H} NMR (200 MHz, [D$_8$]toluene, 25°C): δ=142.42 (m, *i*-C), 130.05 (t, *o*-C), 128.49 (s, *p*-C), 127.70 (s, *m*-C), 40.99 (t, J^1_{PC}=89.9 Hz, CNa_2P_2), 4.32 ppm (s, CH_3Si); ^{31}P{^{1}H} NMR (121 MHz, [D$_8$]toluene, 25°C): δ=7.56 ppm; ^{29}Si NMR (99 MHz, [D$_8$]toluene, 25°C): δ=−15.35 (t, $J^2_{P\text{-}Si}$=8.5 Hz); IR (Nujol mull): $\tilde{\nu}$=1303(w), 1256(m), 1242(m), 1159(w), 1104(m), 1085(m), 1028(w), 976(w), 849(m), 827(m), 742(m), 721(m), 696(m), 672(w), 645(w), 593(w), 557(w), 534(w), 510(w) cm^{-1}.

[({Ph$_2$P(NSiMe$_3$)}$_2$CLiNa)$_2$], 4: The phosphinimine (0.559 g, 1.0 mmol) was dissolved in dry benzene (10 mL), and *t*BuLi (1.70 M, 1.24 mL, 2.1 mmol) was then added slowly to the solution at ambient temperature. The resulting yellow mixture was stirred for 1.5 h (the formation of dilithio **1** was confirmed by in situ ^{1}H NMR studies). *t*BuONa (0.211 g, 2.2 mmol) was then added slowly to the mixture through a solids addition tube. The volume of the solution was reduced in vacuo until precipitation ensued. The mixture was then heated to afford a clear yellow solution. Cooling to ambient temperature resulted in the formation of pale yellow crystals (isolated yield: 0.303 g, 52%). The resulting compound was highly air-sensitive and required manipulation inside an argon-filled glove box. The crystals decomposed without melting above 200°C. The complex crystallizes with two benzene molecules per dimer, as determined by X-ray crystallography. These molecules are partially removed on evacuation. NMR analyses were complicated because of the co-existence of multiple solution species. Thus, only the major signals discernible for **4** are given. ^{1}H NMR (500 MHz, [D$_8$]toluene, 25°C): δ=7.51 (m, 16H; *o*-H, Ph), 6.96 (m, 24H; *m*-, *p*-H, Ph), 0.09 ppm (s, 36H; CH_3Si); ^{13}C{^{1}H} NMR not assigned due to multiple broad overlapping signals; ^{31}P{^{1}H} NMR (121 MHz, [D$_8$]toluene, 25°C): δ=14.60 ppm; ^{29}Si NMR (99 MHz, [D$_8$]toluene, 25°C): δ=−12.86 ppm (t, $J^2_{P\text{-}Si}$=7.73 Hz); ^{7}Li NMR (194 MHz, [D$_8$]toluene, 25°C): δ=0.58 ppm; IR (Nujol mull): $\tilde{\nu}$=1304(w), 1258(w), 1243(w), 1199(w), 1174(w), 1107(m), 1084(m), 1026(w), 848(m), 828(m), 759(w), 740(w), 724(w), 702(w), 645(w), 592(w), 536(w), 507(w) cm^{-1}.

[({Ph$_2$P(NSiMe$_3$)}$_2$C)$_2$LiNa$_3$], 5: The phosphinimine (0.559 g, 1.0 mmol) was dissolved in dry benzene (10 mL) and *n*BuNa (0.120 g, 1.5 mmol) was then added slowly to the solution at ambient temperature through a solids addition tube. The resulting yellow mixture was stirred for 30 min. *t*BuLi (1.70 M, 0.294 mL, 0.5 mmol) was then added slowly to the mixture. The volume of the solution was reduced in vacuo until precipitation ensued. The mixture was then heated to afford a clear orange solution. Cooling to ambient temperature resulted in the formation of yellow crystals. The resulting compound was highly air-sensitive and required manipulation inside an argon-filled glove box. The complex crystallizes with two benzene molecules per dimer, as determined by X-ray crystallography. Further analytical analyses were complicated owing to the co-crystallization of **5** with **3** and **4**, and also as multiple species are established in solution. Spiking experiments in [D$_8$]toluene determined the characteristic ^{1}H NMR Me_3Si signal to be located at δ=0.03 ppm.

[({Ph$_2$P(NSiMe$_3$)}$_2$CLiK)$_2$], 6: The phosphinimine (0.559 g, 1.0 mmol) was dissolved in dry benzene (10 mL) and *t*BuLi (1.70 M, 1.24 mL, 2.1 mmol) was then added slowly to the solution at ambient temperature. The resulting yellow mixture was stirred for 1.5 h. *t*BuOK (0.247 g, 2.2 mmol) was then added slowly to the mixture through a solids addition tube. The volume of the solution was reduced in vacuo until precipitation ensued. The mixture was then heated to afford a clear red-orange solution. Cooling to ambient temperature resulted in the formation of yellow crystals (isolated yield: 0.175 g, 29%). The resulting compound was highly air-sensitive and required manipulation inside an argon-filled glove box. The crystals decomposed without melting above 200°C. ^{1}H NMR (300 MHz, [D$_8$]toluene, 25°C): δ=7.73–7.62 (br s, 16H; *o*-H, Ph), 7.10–6.88 (br s, 24H; *m*-, *p*-H, Ph), 0.23 ppm (s, 36H; CH_3Si); ^{13}C{^{1}H} NMR (75.43 MHz, [D$_8$]toluene, 25°C): δ=143.31 (m, *i*-C), 131.41 (br s, *o*-C), 128.50 (s, *p*-C), 127.48, 126.96 (t, *m*-C), 5.57 ppm (s, CH_3Si); ^{31}P{^{1}H} NMR (121 MHz, [D$_8$]toluene, 25°C): δ=6.71 ppm; ^{29}Si NMR (99 MHz, [D$_8$]toluene, 25°C): δ=−16.44 ppm (t, $J^2_{P\text{-}Si}$=9.33 Hz); ^{7}Li NMR (194 MHz, [D$_8$]toluene, 25°C): δ=0.22; IR (Nujol mull): $\tilde{\nu}$=1304(w), 1253(m), 1242(m), 1206(m), 1174(w), 1118(s), 1086(s), 1027(w), 974(w), 850(s), 825(s), 756(m), 741(m), 725(s), 701(s), 674(w), 646(m), 619(w), 589(m), 535(s), 508(m) cm^{-1}.

[{({Ph$_2$P(NSiMe$_3$)}$_2$C)NaK}$_2$], 7: The phosphinimine (0.559 g, 1.0 mmol) was dissolved in dry benzene (10 mL) and *n*BuNa (0.168 g, 2.1 mmol) was then added slowly to the solution through a solids addition tube at ambient temperature. The resulting yellow mixture was stirred for 30 min (the formation of disodio **3** was confirmed by in situ ^{1}H NMR studies). *t*BuOK (0.247 g, 2.2 mmol) was then added slowly to the mixture through a solids addition tube. The volume of the solution was reduced in vacuo until precipitation ensued. The mixture was then heated to afford a clear red-orange solution. Cooling to ambient temperature resulted in the formation of yellow crystals (isolated yield: 0.182 g, 29.4%). The resulting compound was highly air-sensitive and required manipulation inside an argon-filled glove box. The crystals decomposed without melting above 180°C. The complex crystallizes with two benzene molecules per dimer, as determined by X-ray crystallography. ^{1}H NMR (300 MHz, [D$_8$]toluene, 25°C): δ=7.81–7.27 (br s, 16H; *o*-H, Ph), 6.96 (m, 24H; *m*-, *p*-H, Ph), 0.12 ppm (s, 36H; CH_3Si); ^{13}C{^{1}H} NMR (200 MHz, [D$_8$]toluene, 25°C): δ=145.09 (t, *i*-C), 127.91 (t, *o*-C), 131.06 (s, *p*-C), 127.28 (s, *m*-C), 38.04 (t, J^1_{PC}=106.32 Hz, $CNaP_2$), 5.50 ppm (s, CH_3Si); ^{31}P{^{1}H} NMR (121 MHz, [D$_8$]toluene, 25°C): δ=3.95 ppm; ^{29}Si NMR (99 MHz, [D$_8$]toluene, 25°C): δ=−19.94 ppm (t, $J^2_{P\text{-}Si}$=9.78 Hz); IR (Nujol mull): $\tilde{\nu}$=1303(w), 1257(m), 1242(m), 1200(m), 1124(s), 1087(m), 1026(w), 974(w), 848(s), 822(s), 738(m), 722(s), 699(s), 643(w), 529(m), 508(m) cm^{-1}.

[({Ph$_2$P(NSiMe$_3$)}$_2$C)$_2$Na$_3$K], 8: The monopotassiated compound **12** (0.597 g, 1.0 mmol) was dissolved in dry benzene (10 mL) and *n*BuNa (0.120 g, 1.5 mmol) was then added slowly to the solution through a solids addition tube at ambient temperature. The resulting yellow mixture was stirred for 30 min. The volume of the solution was reduced in vacuo until precipitation ensued. The mixture was then heated to afford a clear red-orange solution. Cooling to ambient temperature resulted in the formation of yellow crystals. The resulting compound was highly air-sensitive and required manipulation inside an argon-filled glove box. The complex crystallizes with two benzene molecules per dimer, as determined by X-ray crystallography.

[{Ph$_2$P(NSiMe$_3$)}$_2$CH}{(Me$_3$Si)$_2$N}NaK·Tol], 9: The phosphinimine (0.559 g, 1.0 mmol) was dissolved in dry toluene (10 mL) and NaHMDS (0.202 g, 1.1 mmol) was then added slowly to the solution through a solids addition tube at ambient temperature. The resulting colorless mixture was stirred for 1 h. BnK (0.143 g, 1.1 mmol) was then added slowly through a solids addition tube. The resulting yellow solution was stirred for 1 h. The volume of the solution was reduced in vacuo until precipitation ensued. The mixture was then heated to afford a clear yellow solution. Cooling to ambient temperature resulted in the formation of colorless crystals. The resulting compound was air-sensitive and required manipulation inside an argon-filled glove box. ^{1}H NMR (300 MHz, [D$_8$]toluene, 25°C): δ=7.75 (d, 8H; *o*-H, Ph), 7.09–6.97 (m, 12H; *m*-, *p*-H, Ph), 1.72 (t, 1H; $CHNaP_2$), 0.092 (s, 18H; CH_3Si), 0.088 ppm (s, 18H; CH_3Si); ^{13}C{^{1}H} NMR (200 MHz, [D$_8$]toluene, 25°C): δ=142.77 (d, $^1J_{PC}$=95.37 Hz, *i*-C), 131.32 (t, $^2J_{PC}$=5.13 Hz, *o*-C), 129.05 (s, *p*-C), 127.72 (t, $^3J_{PC}$=5.50 Hz, *m*-C), 25.98 (t, J^1_{PC}=131.32 Hz, $CHNaP_2$), 7.08 (s, N-($SiMe_3$)$_2$), 4.74 ppm (s, CH_3Si).

Acknowledgement

We gratefully acknowledge the National Science Foundation for support (CHE03-45713 and CHE07-17593). We also thank the National Science Foundation for instrumentation support (CHE04-43233). We also thank Professor William Boggess and the Center for Environmental Science and Technology at Notre Dame for the use of the Micromass Quatro-LC.

[1] K. Ziegler, K. Nagel, M. Patheiger, *Z. Anorg. Allg. Chem.* **1955**, *282*, 345–351.
[2] a) P. A. Carney, I. C. Memco, *J. Am. Chem. Soc.* **1965**, *87*, 3788–3789; b) R. West, P. C. Jones, *J. Am. Chem. Soc.* **1969**, *91*, 6156–6161; c) G. A. Gornowicz, R. West, *J. Am. Chem. Soc.* **1971**, *93*, 1714–1720; d) G. A. Gornowicz, R. West, *J. Am. Chem. Soc.* **1971**, *93*, 1720–1724; e) W. Priester, R. West, T. L. Chwang, *J. Am. Chem. Soc.* **1976**, *98*, 8413–8421.
[3] a) C. Chung, R. J. Lagow, *J. Chem. Soc. Chem. Commun.* **1972**, 1078–1079; b) L. A. Shimp, R. J. Lagow, *J. Am. Chem. Soc.* **1973**, *95*, 1343–1344; c) J. A. Morrison, C. Chung, R. J. Lagow, *J. Am. Chem. Soc.* **1975**, *97*, 5015–5017; d) L. A. Shimp, R. J. Lagow, *J. Am. Chem. Soc.* **1979**, *101*, 2214–2216.
[4] K. C. Eberly, H. E. Adams, *J. Organomet. Chem.* **1965**, *3*, 165–167.
[5] P. L. Timms, *Angew. Chem.* **1975**, *87*, 295–299; *Angew. Chem. Int. Ed. Engl.* **1975**, *14*, 273–277.
[6] a) I. Marek, J. F. Normant, *Chem. Rev.* **1996**, *96*, 3241–3267; b) I. Marek, *Chem. Rev.* **2000**, *100*, 2887–2900; c) J. F. Normant, *Acc. Chem. Res.* **2001**, *34*, 640–644.
[7] a) J. F. K. Müller, *Eur. J. Inorg. Chem.* **2000**, 789–799; b) C. Strohmann, D. Schildbach in *The Chemistry of Organolithium Compounds* (Eds.: Z. Rappoport, I. Marek) Chichester, Wiley, **2004**, pp. 941.
[8] J. B. Collins, J. D. Dill, E. D. Jemmis, Y. Apeloig, P. v. R. Schleyer, R. Seeger, J. A. Pople, *J. Am. Chem. Soc.* **1976**, *98*, 5419–5427.
[9] a) W. D. Laidig, H. F. Schaefer, *J. Am. Chem. Soc.* **1978**, *100*, 5972–5973; b) E. D. Jemmis, P. v. R. Schleyer, J. A. Pople, *J. Organomet. Chem.* **1978**, *154*, 327–335; c) S. M. Bachrach, A. Streitwieser, *J. Am. Chem. Soc.* **1984**, *106*, 5818–5824; d) J. P. Ritchie, S. M. Bachrach, *J. Am. Chem. Soc.* **1987**, *109*, 5909–5916; e) A. E. Alvarado-Swaisgood, *Diss. Abstr. Int. B* **1987**,*47*, 4892.
[10] J. A. Gurak, J. W. Chinn Jr., R. J. Lagow, *J. Am. Chem. Soc.* **1982**, *104*, 2637–2639.
[11] J. A. Gurak, J. W. Chinn, Jr., R. J. Lagow, H. Steinfink, C. S. Yannoni, *Inorg. Chem.* **1984**, *23*, 3717–3720.
[12] G. D. Stucky, M. M. Eddy, W. H. Harrison, R. Lagow, H. Kawa, D. E. Cox, *J. Am. Chem. Soc.* **1990**, *112*, 2425–2427.
[13] T. Swanson, *NBS Monogr. (U.S.)* **1962**, No. 25, 1.
[14] R. Stackelberg, V. Quatram, *Z. Phys. Chem.* **1934** *B27*, 50–52.
[15] K. L. Hull, B. C. Noll, K. W. Henderson, *Organometallics* **2006**, *25*, 4072–4074.
[16] A. Kasani, R. P. Kamalesh Babu, R. McDonald, R. G. Cavell, *Angew. Chem.* **1999**, *111*, 1580–1582; *Angew. Chem. Int. Ed.* **1999**, *38*, 1483–1484.
[17] C. M. Ong, D. W. Stephan, *J. Am. Chem. Soc.* **1999**, *121*, 2939–2940.
[18] W. Zarges, M. Marsch, K. Harms, G. Boche, *Chem. Ber.* **1989**, *122*, 1307–1311.
[19] G. Linti, A. Rodig, H. Pritzkow, *Angew. Chem.* **2002**, *114*, 4685–4687; *Angew. Chem. Int. Ed.* **2002**, *41*, 4503–4506.
[20] T. Cantat, L. Ricard, P. Le Floch, N. Mézailles, *Organometallics* **2006**, *25*, 4965–4976.
[21] H. J. Gais, J. Vollhardt, H. Günther, D. Moskau, H. J. Lindner, S. Braun, *J. Am. Chem. Soc.* **1988**, *110*, 978–980.
[22] J. F. K. Müller, M. Neuburger, B. Spingler, *Angew. Chem.* **1999**, *111*, 3766–3769; *Angew. Chem. Int. Ed.* **1999**, *38*, 3549–3552.
[23] J. F. K. Müller, M. Neuburger, B. Spingler, *Angew. Chem.* **1999**, *111*, 97–99; *Angew. Chem. Int. Ed.* **1999**, *38*, 92–94.
[24] A. Muller, B. Neumuller, K. Dehnicke, J. Magull, D. Fenske, *Z. Anorg. Allg. Chem.* **1997**, *623*, 1306–1310.
[25] W. Uhl, M. Layh, W. Massa, *Chem. Ber.* **1991**, *124*, 1511–1516.
[26] a) K. W. Henderson, A. R. Kennedy, A. E. McKeown, D. S. Strachan, *J. Chem. Soc. Dalton Trans.* **2000**, 4348–4353; b) K. W. Henderson, A. R. Kennedy, D. J. MacDougall, D. Shanks, *Organometallics* **2002**, *21*, 606–616; c) K. W. Henderson, A. R. Kennedy, D. J. MacDougall, *Inorg. Chem.* **2003**, *42*, 2736–2741; d) D. J. MacDougall, A. R. Kennedy, B. C. Noll, K. W. Henderson, *Dalton Trans.* **2005**, 2084–2091.
[27] P. J. Crowley, M. R. Leach, O. Meth-Cohn, B. J. Wakefield, *Tetrahedron Lett.* **1986**, *27*, 2909–2912.
[28] W. Zarges, M. Marsch, K. Harms, G. Boche, *Angew. Chem.* **1989**, *101*, 1424–1425; *Angew. Chem. Int. Ed. Engl.* **1989**, *28*, 1392–1394.
[29] a) J. B. Collins, J. D. Dill, E. D. Jemmis, Y. Apeloig, P. v. R. Schleyer, R. Seeger, J. A. Pople, *J. Am. Chem. Soc.* **1976**, *98*, 5419–5427; b) A. Mavridis, J. F. Harrison, J. F. Liebman, *J. Phys. Chem.* **1984**, *88*, 4973–4978; c) X. E. Zheng, Z. Z. Wang, A. C. Tang, *J. Mol. Struct. (Theochem.)* **1999**, *492*, 105–111.
[30] C. M. Thomson, *Dianion Chemistry in Organic Synthesis*, CRC Press, Boca Raton, **1994**.
[31] A. Müller, M. Möhlen, B. Neumüller, N. Faza, W. Massa, K. Dehnicke, *Z. Anorg. Allg. Chem.* **1999**, *625*, 1748–1751.
[32] K. Aparna, R. McDonald, M. Ferguson, R. G. Cavell, *Organometallics* **1999**, *18*, 4241–4243.
[33] W. P. Leung, Z. X. Wang, H. W. Li, T. C. W. Mak, *Angew. Chem.* **2001**, *113*, 2569–2571; *Angew. Chem. Int. Ed.* **2001**, *40*, 2501–2503.
[34] A. Kasani, R. McDonald, R. G. Cavell, *Chem. Commun.*, **1999**, 1993–1994.
[35] T. Bollwein, M. Westerhausen, A. Pfitzner, *Z. Naturforsch. B* **2003**, *58* 493–495.
[36] M. Fang, N. D. Jones, R. Lukowski, J. Tjathas, M. J. Ferguson, R. G. Cavell, *Angew. Chem.* **2006**, *118*, 3169–3173; *Angew. Chem. Int. Ed.* **2006**, *45*, 3097–3101.
[37] N. D. Jones, G. Lin, R. A. Gossage, R. McDonald, R. G. Cavell, *Organometallics* **2003**, *22*, 2832–2841.
[38] R. G. Cavell, R. P. K. Babu, A. Kasani, R. McDonald, *J. Am. Chem. Soc.* **1999**, *121*, 5805–5806.
[39] a) M. T. Gamer, M. Rastatter, P. W. Roesky, *Z. Anorg. Allg. Chem.* **2002**, *628*, 2269–2272; b) M. T. Gamer, P. W. Roesky, *Z. Anorg. Allg. Chem.* **2001**, *627*, 877–881.
[40] K. Aparna, M. Ferguson, R. G. Cavell, *J. Am. Chem. Soc.* **2000**, *122*, 726–727.
[41] R. P. Kamalesh Babu, R. McDonald, R. G. Cavell, *Organometallics* **2000**, *19*, 3462–3465.
[42] W. P. Leung, C. W. So, Z. X. Wang, T. C. W. Mak, *Chem. Commun.* **2003**, 248–249.
[43] W. P. Leung, C. W. So, Z. X. Wang, J. Z. Wang, T. C. W. Mak, *Organometallics* **2003**, *22*, 4305–4311.
[44] W. P. Leung, C. W. So, K. W. Kan, H. S. Chan, T. C. W. Mak, *Inorg. Chem.* **2005**, *44*, 7286–7288.
[45] a) L. Orzechowski, G. Jansen, S. Harder, *J. Am. Chem. Soc.* **2006**, *128*, 14676–14684; b) L. Orzechowski, S. Harder, *Organometallics* **2007**, *26*, 2144–2148.
[46] L. Orzechowski, S. Harder, *Organometallics* **2007**, *26*, 5501–5506.
[47] a) R. P. Kamalesh Babu, K. Aparna, R. McDonald, R. G. Cavell, *Inorg. Chem.* **2000**, *39*, 4981–4984; b) R. P. Kamalesh Babu, A. Kasani, R. McDonald, R. Cavell, *Organometallics* **2001**, *20*, 1451–1455.
[48] L. Lochmann, J. Pospišil, D. Lim, *Tetrahedron Lett.* **1966**, *7*, 257–262.
[49] T. R. Hoye, A. W. Aspaas, B. M. Eklov, T. D. Ryba, *Org. Lett.* **2005**, *7*, 2205–2208.
[50] a) T. Stey, D. Stalke in *The Chemistry of Organolithium Compounds* (Eds.: Z. Rappoport, S. Patai) New York, Wiley, **2004**, Chapter 2; b) E. Weiss, *Angew. Chem. Int. Ed. Engl.* **1993**, *32*, 1501–1523; c) *Lithium Chemistry, A Theoretical and Experimental Overview* (Eds.: A. M. Sapse, P. v. R. Schleyer) New York, John Wiley & Sons, **1995**.
[51] For a discussion on cation-π interactions see: a) J. J. Morris, B. C. Noll, G. W. Honeyman, C. T. O'Hara, A. R. Kennedy, R. E. Mulvey, K. W. Henderson, *Chem. Eur. J.*, **2007**, *13*, 4418–4432; b) J. B. Ran-

dazzo, J. J. Morris, K. W. Henderson, *Main Group Chem.* **2006**, *5*, 215–220.
[52] C. Lambert, P. v. R. Schleyer, *Angew. Chem.* **1994**, *106*, 1187–1199; *Angew. Chem. Int. Ed. Engl.* **1994**, *33*, 1129–1140.
[53] M. Klobukowski, S. A. Decker, C. C. Lovallo, R. G. Cavell, *THEOCHEM* **2001**, *536*, 189–194.
[54] For a related study of monometalated iminophosphorane see: N. Kocher, D. Leusser, A. Murso, D. Stalke, *Chem. Eur. J.* **2004**, *10*, 3622–3631.
[55] W. Scherer, P. Sirsch, D. Shorokhov, G. S. McGrady, S. A. Mason, M. G. Gardiner, *Chem. Eur. J.* **2002**, *8*, 2324–2334.
[56] D. F. Shriver, M. A. Drezdzon *Manipulation of Air Sensitive Compounds*, New York John Wiley and Sons, **1986**.
[57] Bruker-Nonius AXS (**2005**). APEX2 and COSMO. Bruker-Nonius AXS, Madison, Wisconsin, USA.
[58] G. M. Sheldrick, University of Göttingen, Göttingen (Germany), **2004**.
[59] G. M. Sheldrick, SHELXTL. Bruker-Nonius AXS, Madison, Wisconsin, USA, **2001**.
[60] Gaussian 03, Revision C.02, M. J. Frisch, G. W. Trucks, H. B. Schlegel, G. E. Scuseria, M. A. Robb, J. R. Cheeseman, J. A. Montgomery, Jr., T. Vreven, K. N. Kudin, J. C. Burant, J. M. Millam, S. S. Iyengar, J. Tomasi, V. Barone, B. Mennucci, M. Cossi, G. Scalmani, N. Rega, G. A. Petersson, H. Nakatsuji, M. Hada, M. Ehara, K. Toyota, R. Fukuda, J. Hasegawa, M. Ishida, T. Nakajima, Y. Honda, O. Kitao, H. Nakai, M. Klene, X. Li, J. E. Knox, H. P. Hratchian, J. B. Cross, C. Adamo, J. Jaramillo, R. Gomperts, R. E. Stratmann, O. Yazyev, A. J. Austin, R. Cammi, C. Pomelli, J. W. Ochterski, P. Y. Ayala, K. Morokuma, G. A. Voth, P. Salvador, J. J. Dannenberg, V. G. Zakrzewski, S. Dapprich, A. D. Daniels, M. C. Strain, O. Farkas, D. K. Malick, A. D. Rabuck, K. Raghavachari, J. B. Foresman, J. V. Ortiz, Q. Cui, A. G. Baboul, S. Clifford, J. Cioslowski, B. B. Stefanov, G. Liu, A. Liashenko, P. Piskorz, I. Komaromi, R. L. Martin, D. J. Fox, T. Keith, M. A. Al-Laham, C. Y. Peng, A. Nanayakkara, M. Challacombe, P. M. W. Gill, B. Johnson, W. Chen, M. W. Wong, C. Gonzalez, and J. A. Pople, Gaussian, Wallingford CT, **2004**.
[61] A. D. Becke, *J. Chem. Phys.* **1993**, *98*, 5648–5652.
[62] a) P. C. Hariharan, J. A. Pople, *Theo. Chim. Acta* **1973**, *28*, 213–222; b) M. M. Francl, W. J. Pietro, W. J. Hehre, J. S. Binkley, D. J. DeFrees, J. A. Pople, M. S. Gordon, *J. Chem. Phys.* **1982**, *77*, 3654–3665; c) V. A. Rassolov, J. A. Pople, M. A. Ratner, T. L. Windus, *J. Chem. Phys.* **1998**, *109*, 1223–1229.
[63] a) R. Krishnan, J. S. Binkley, R. Seeger, J. A. Pople, *J. Chem. Phys.* **1980**, *72*, 650–654; b) J. P. Blaudeau, M. P. McGrath, L. A. Curtiss, L. Radom, *J. Chem. Phys.* **1997**, *107*, 5016–5021.
[64] J. E. Carpenter, F. Weinhold, *THEOCHEM* **1988**,*169*, 41–62.
[65] a) A. E. Reed, F. Weinhold, *J. Chem. Phys.* **1983**, *78*, 4066–4073; b) A. E. Reed, R. B. Weinstock, F. Weinhold, *J. Chem. Phys.* **1985**, *83*, 735–746.

Received: December 14, 2007
Published online: March 20, 2008

